JGP Journal of General Physiology

RESEARCH ARTICLE

Phenotypic plasticity in *Periplaneta americana* photoreceptors

Roman V. Frolov[1], Esa-Ville Immonen[1], Paulus Saari[1], Päivi H. Torkkeli[2], Hongxia Liu[2], and Andrew S. French[2]

Plasticity is a crucial aspect of neuronal physiology essential for proper development and continuous functional optimization of neurons and neural circuits. Despite extensive studies of different visual systems, little is known about plasticity in mature microvillar photoreceptors. Here we investigate changes in electrophysiological properties and gene expression in photoreceptors of the adult cockroach, *Periplaneta americana,* after exposure to constant light (CL) or constant dark (CD) for several months. After CL, we observed a decrease in mean whole-cell capacitance, a proxy for cell membrane area, from 362 ± 160 to 157 ± 58 pF, and a decrease in absolute sensitivity. However, after CD, we observed an increase in capacitance to 561 ± 155 pF and an increase in absolute sensitivity. Small changes in the expression of light-sensitive channels and signaling molecules were detected in CD retinas, together with a substantial increase in the expression of the primary green-sensitive opsin (GO1). Accordingly, light-induced currents became larger in CD photoreceptors. Even though normal levels of GO1 expression were retained in CL photoreceptors, light-induced currents became much smaller, suggesting that factors other than opsin are involved. Latency of phototransduction also decreased significantly in CL photoreceptors. Sustained voltage-activated K^+ conductance was not significantly different between the experimental groups. The reduced capacitance of CL photoreceptors expanded their bandwidth, increasing the light-driven voltage signal at high frequencies. However, voltage noise was also amplified, probably because of unaltered expression of TRPL channels. Consequently, information transfer rates were lower in CL than in control or CD photoreceptors. These changes in whole-cell capacitance and electrophysiological parameters suggest that structural modifications can occur in the photoreceptors to adapt their function to altered environmental conditions. The opposing patterns of modifications in CL and CD photoreceptors differ profoundly from previous findings in *Drosophila melanogaster* photoreceptors.

Introduction

Environmental stimuli contribute to the proper development and maintenance of sensory receptors and their downstream neural circuits. In visual systems, the effects of such stimulation, or its lack, can range from a failure to establish proper synaptic connections during ontogenesis (Hubel and Wiesel, 1970; Hubel et al., 1977; Jiang et al., 2009) to various forms of synaptic plasticity (Berry and Nedivi, 2016; Pallas, 2017). For peripheral visual systems, numerous short- and long-term activity–dependent modifications have been described over different time scales at both the cellular and network levels in photoreceptors and higher-order visual neurons (Brann and Cohen, 1987; Sokolov et al., 2002; Wagner and Kröger, 2005; Calvert et al., 2006).

Studies of plasticity in invertebrate visual systems have examined developmental changes at the first visual synapse, connections between neurons in the higher-order visual centers (Hertel, 1983; Meinertzhagen, 1989; Barth et al., 1997; Pallas, 2017), short-term light adaptations in the retina (Laughlin, 1989), and illumination-dependent changes at the molecular level in photoreceptors (Bähner et al., 2002; Cronin et al., 2006; Frechter and Minke, 2006). However, little is known about long-term functional adaptations in microvillar photoreceptors. Phenotypic plasticity of the electrophysiological properties of microvillar photoreceptors has primarily been explored in dipterans. Vision of the housefly, *Musca domestica*, displayed improved absolute sensitivity and contrast sensitivity when it was reared in complete darkness for several days after emergence (Deimel and Kral, 1992). When the fruit fly, *Drosophila melanogaster*, was exposed to light, its photoreceptor responses were faster and less noisy, with higher information capacity than in dark-reared flies (Wolfram and Juusola, 2004; Voolstra et al., 2017). In addition, long-term changes in the K^+ current of the sea slug *Hermissenda*

[1]Biophysics group, Nano and Molecular Systems Research Unit, University of Oulu, Oulu, Finland; [2]Department of Physiology and Biophysics, Dalhousie University, Halifax, NS, Canada.

Correspondence to Roman V. Frolov: rvfrolov@gmail.com.

© 2018 Frolov et al. This article is distributed under the terms of an Attribution–Noncommercial–Share Alike–No Mirror Sites license for the first six months after the publication date (see http://www.rupress.org/terms/). After six months it is available under a Creative Commons License (Attribution–Noncommercial–Share Alike 4.0 International license, as described at https://creativecommons.org/licenses/by-nc-sa/4.0/).

Downloaded from http://rupress.org/jgp/article-pdf/150/10/1386/1797456/jgp_201812107.pdf by guest on 09 February 2026

crassicornis photoreceptors were detected after relatively short exposure to light (Yamoah et al., 2005).

Although most research into invertebrate vision has been performed in flies, their photoreceptors are different from many other microvillar photoreceptors. The fly visual system is evolutionarily tuned to operate with relatively high speeds of movement and maneuvering (Weckström and Laughlin, 1995; Frolov et al., 2016). Their compound eyes are characterized by open-rhabdom organization of the ommatidia, with neural superposition taking place in the first optic ganglion, the lamina (Fain et al., 2010). In contrast to hemimetabolous insect species, where photoreceptors must function while they grow during a period of postembryonic development (Frolov et al., 2012), adult fly photoreceptors do not grow. They become functionally mature during the first hours or days after eclosion (Rudolf et al., 2014). Also, the relatively short life spans of flies (Carey, 2001) preclude prolonged light exposure/deprivation experiments. Also, our recent analyses of phototransduction in the cockroach *Periplaneta americana*, including knockdown of several retinal proteins by RNA interference, have suggested that the phototransduction cascades of flies and cockroaches differ in several important aspects, including the role of Ca^{2+} and expression patterns of light-activated channels (Immonen et al., 2014, 2017; French et al., 2015; Saari et al., 2017).

Here, we investigated photoreceptors of adult *P. americana* that were reared in uniform bright light or darkness for several months. Electrophysiological recordings from photoreceptors in dissociated ommatidia revealed distinct and opposing physiological adaptations that suggest morphological changes compared with photoreceptors of control animals maintained under normal illumination (12 h light:12 h dark) conditions. These changes are likely to involve structural remodeling of light-sensitive membrane but also affect the timing of phototransduction. We argue that these changes adjust photoreceptor function to different illumination conditions.

Materials and methods

American cockroaches, *P. americana* (Linnaeus), were purchased from Blades Biological and maintained at 25°C under three light regimens: in constant light (CL), in reversed 12-h/12-h illumination conditions with a subjective "night" period matching the actual day (control), and in nearly constant dark (CD). Illumination for the CL group and for the subjective day period of control groups was provided by the built-in incubator light source and corresponded to bright indoor illumination (~2,000 lux). CL cockroaches were housed in individual transparent cages with a cardboard shelter available. CD cockroaches were housed in a large Plexiglas container with plenty of shelter available and were occasionally and briefly exposed to room light during servicing. Only male cockroaches were used for experiments.

Patch-clamp recordings

Ommatidia were dissociated, and whole-cell recordings were performed as described previously (Saari et al., 2017). In brief, data were acquired using an Axopatch 1-D patch-clamp amplifier, Digidata 1550 digitizer, and pClamp 10 software (Axon Instruments/Molecular Devices). Patch electrodes were made from a thin-walled borosilicate glass (World Precision Instruments) and had resistances of 4–9 MΩ. Bath solution contained (in mM) 120 NaCl, 5 KCl, 4 $MgCl_2$, 1.5 $CaCl_2$, 10 *N*-Tris-(hydroxymethyl)-methyl-2-amino-ethanesulfonic acid (TES), 25 proline, and 5 alanine, pH 7.15. Patch pipette solution contained (in mM) 100 K-gluconate, 40 KCl, 10 TES, 2 $MgCl_2$, 4 Mg-ATP, 0.4 Na-GTP, and 1 NAD, pH 7.15. The liquid junction potential (LJP) was −12 mV. All voltage values cited in the text were corrected for the LJP. The series resistance was compensated by 80%. Membrane capacitance was calculated from the total charge flowing during capacitive transients for voltage steps from −112 to −92/−82 mV.

Light stimulation was performed as described previously (Saari et al., 2017). Stimulus intensity was attenuated with a series of neutral-density filters (Kodak). The highest light intensity achievable in our experiments was 10 (arbitrary units), corresponding to bright room illumination. Light intensities in text and figures are presented with dimensionless numbers; e.g., 5×10^{-6} intensity is 2×10^6 lower than the maximal intensity.

Only green-sensitive photoreceptors, which showed stable resting potential ≤−45 mV and light responses, were used for analysis. Recordings were performed at room temperature (20–22°C) during the subjective night of the control group.

Quantification of mRNA expression

Relative expression levels of mRNA were determined by real-time quantitative PCR as described previously (French et al., 2015). In brief, total RNA was extracted from 14–20 retinas from each experimental group, using a RNeasy Plus mini kit (Qiagen). mRNA was evaluated using an Experion RNA Analysis kit (Bio-Rad). 50 ng total RNA was used for first-strand cDNA synthesis with ProtoScript II reverse transcription (New England BioLabs). Quantitative PCR was performed using GoTaq qPCR Master (Promega) on a CFX96TM real-time PCR detection system (Bio-Rad). All PCR runs were performed three times. Gene expression levels, PCR efficiency, and the standard error of measurement were calculated using CFX Manager (Bio-Rad). Primer sequences for the specific and reference genes are provided elsewhere (French et al., 2015). Amplification efficiencies of the primers were determined using serially diluted cDNA samples.

Data analysis

To determine the information transfer rate, we used a 60-s stimulus consisting of 30 repetitions of a 2-s Gaussian white noise (GWN) sequence, with mean contrast of 0.36 and a 3-dB cutoff frequency (f_{3dB}) of 50 Hz. The GWN sequence was preceded by an adapting 0.5-s steady light interval of the same mean intensity to accommodate the initial transient. Data analysis was done in Matlab (MathWorks) as described previously (Frolov, 2015). In brief, a 2-s signal $S(t)$ was obtained by averaging voltage responses to 30 repetitions of the 2-s sequence. $S(t)$ was then converted into $S(f)$ by a fast Fourier transformation (FFT). The noise $N(f)$ was then obtained by subtracting the signal estimate from the original (noise-containing) sequences, converting them to spectra by FFT and averaging all 30 noise spectra. The signal gain of voltage responses $|T(f)|$ was calculated by dividing the cross-spectrum of photoreceptor input (GWN contrast, $C(f)$) and output (photore-

Downloaded from http://rupress.org/jgp/article-pdf/150/10/1386/1797456/jgp_201812107.pdf by guest on 09 February 2026

ceptor signal) $S(f)\cdot C^*(f)$, with * denoting the complex conjugate, by the autospectrum of the input $C(f)\cdot C^*(f)$ and taking the absolute value of the resulting frequency response function $T(f)$: $T(f) = S(f)\cdot C^*(f)/C(f)\cdot C^*(f)$. The Shannon information rate (IR) was calculated as $IR = \int\{\log_2[|S(f)|/|N(f)|+1]\}df$ within the frequency range from 1 to 50 Hz.

Experimental design and statistical analysis

At the initial stage of statistical analysis, the Shapiro–Wilk normality test was applied to data samples to determine if they could be analyzed using parametric statistical methods. Data in the samples that did not pass the normality test were presented using medians and interquartile ranges (25% quartile:75% quartile; e.g., Fig. 7 D). To evaluate differences between such samples, the Mann–Whitney U test (MWUT) was used. In Fig. 7, dependencies of information-processing parameters on frequency are shown as median ± median absolute deviation (m.a.d.). The samples that passed the normality test were analyzed with parametric statistical methods as indicated. Such data are presented as mean ± SD and were compared using a two-tailed unpaired t test with unequal variances. Spearman's rank order correlation coefficient (ρ) was used in analyses of correlations. In figures, *, $P < 0.05$; **, $P < 0.01$. Throughout the text, n stands for experimental group size.

Results

Whole-cell capacitance and absolute light sensitivity

Patch-clamp recordings were performed from CL, control, and CD photoreceptors between days 100 and 150 into the different light regimens. Basic electrophysiological properties include resting potential, input resistance, and whole-cell capacitance. Of these three, only whole-cell capacitance (C_m) was significantly different between the experimental groups (Fig. 1, A–C). Mean C_m in CL cockroaches was 2.4 times smaller and in CD cockroaches 1.5 times higher than in control (Fig. 1 A). C_m distributions are shown in Fig. 1 B.

Absolute sensitivity to light was estimated by counting quantum bumps (elementary photoreceptor responses) evoked by continuous low-intensity light stimulation. Bump rates were first obtained at different light intensities and then recalculated for the common light intensity corresponding to 5×10^{-6} light intensity in Fig. 4 B. Absolute sensitivity was strongly reduced in CL and increased in CD photoreceptors in comparison to control (Fig. 1 C). Although a strong positive correlation was found between C_m and absolute sensitivity in control ($\rho = 0.73$, $n = 59$, $P < 10^{-6}$, Fig. 1 C), no statistically significant correlation was found in either CL or CD groups because of relatively small sample sizes.

Quantum bump latency

Next, we tested if prolonged exposure to CL or dark changed the latency of elementary (quantum bumps) and macroscopic responses. Quantum bumps were evoked in voltage-clamp mode by 1-ms flashes of green light of such intensity as to trigger bumps with a probability of <0.7. Bump latency was determined as an interval between the onset of light and the time quantum bump amplitude reached 10% of its maximum value. Fig. 2 (A–C) shows typical responses of CL, control, and CD photoreceptors, respectively, with stimulus given at 0 ms and red dashed lines indicating median bump latencies. Normalized bump latency distributions are shown in Fig. 2 D. Mean bump latency was significantly smaller in CL than in control and CD photoreceptors (Fig. 2 E).

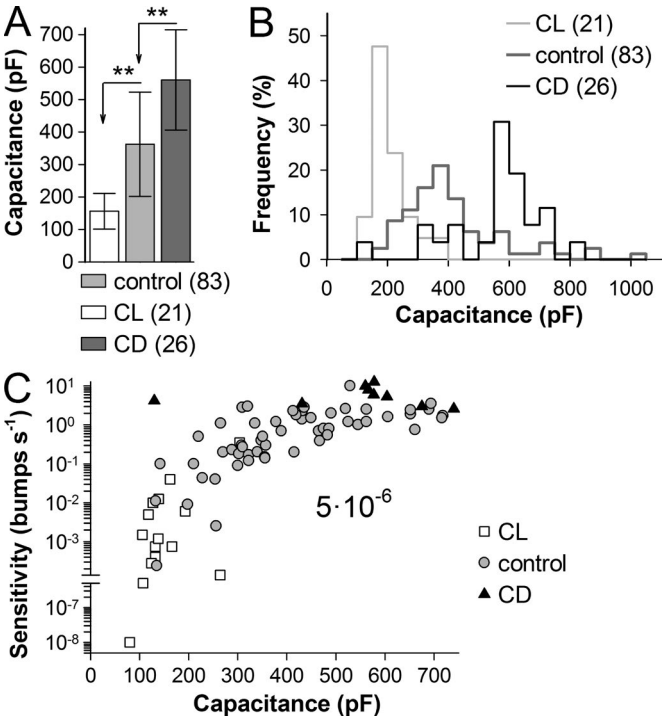

Figure 1. **Changes in photoreceptor capacitance and absolute sensitivity. (A)** Mean capacitance values of photoreceptors in CL, control, and CD; here and elsewhere, n indicates the number of cells, and error bars denote SD. Mean C_m was 157 ± 58 pF in CL ($n = 21$; $P < 10^{-12}$, unpaired t test, comparison with control), 374 ± 180 pF in control ($n = 83$), and 560 ± 149 pF in CD photoreceptors ($n = 26$; $P < 10^{-5}$, unpaired t test, comparison with control). **, $P < 0.01$. **(B)** Distributions of C_m values. **(C)** Correlations between C_m and absolute sensitivity; sensitivity values were determined by counting bump rates in response to continuous stimulation at light intensities evoking <10 bumps/s; the rates were recalculated for the common light intensity 5×10^{-6} as in Fig. 4 B. The median values were 1.2×10^{-3} (0.3×10^{-3}:8.0×10^{-3}) in CL ($n = 15$), 0.75 (0.19:1.85) in control ($n = 59$), and 5.3 (3.5:8.0) bumps/s in CD ($n = 9$) photoreceptors. The differences were highly significant, with $P < 10^{-4}$ (MWUT) for comparisons of both CL and CD groups to control.

Elementary responses

We also compared mean amplitudes and half-widths of current quantum bumps from the three experimental groups. Although there appeared to be differences in mean amplitudes and half-widths, with the smallest mean amplitude and largest mean half-width observed in CD photoreceptors, these differences were not statistically significant and could in principle be explained by large residual uncompensated capacitance in CD but not CL photoreceptors, which slows clamp speed compared with control and especially CL photoreceptors.

Next, we tested if the differences in photoreceptor capacitance altered the amount of low-pass filtering by the membrane. Indeed, dramatic differences in voltage bumps were observed between CL

Downloaded from http://rupress.org/jgp/article-pdf/150/10/1386/1797456/jgp_201812107.pdf by guest on 09 February 2026

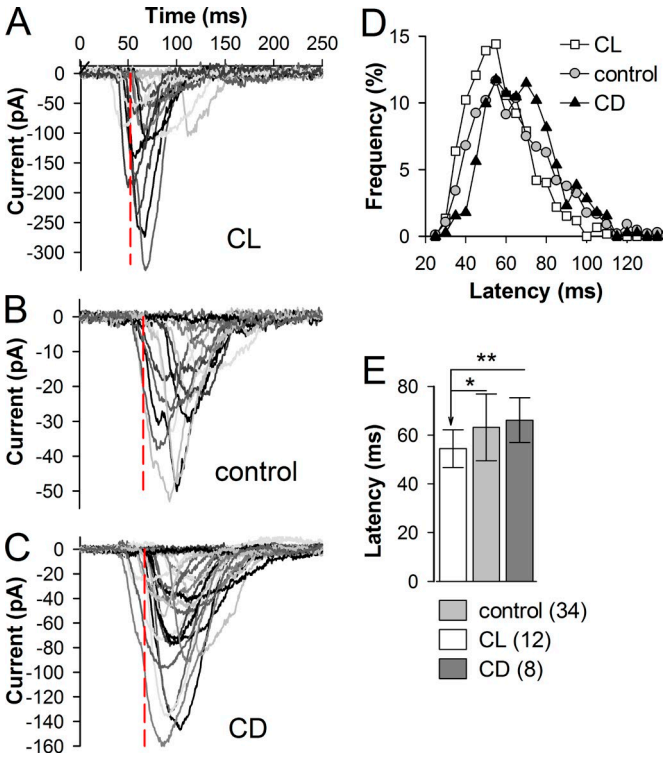

Figure 2. **Photoreceptor latency. (A–C)** Typical responses of CL, control, and CD photoreceptors to 1-ms flashes of light; light intensity was adjusted to evoke quantum bumps with a probability of <70%; stimulus was given at 0 ms; dashed lines indicate bump latency medians for these cells; bump latency was determined as the interval between the onset of light and the time that the quantum bump amplitude reached 10% of its maximum value. **(D)** Normalized distributions of bump latencies; to obtain the distributions, 50 latency values from each cell were combined into a common pool, and frequencies were normalized. **(E)** Mean latency values were obtained by averaging mean latencies from each photoreceptor. Mean bump latency was significantly smaller in CL than in control and CD photoreceptors: the values were 54.4 ± 7.8 ms in CL (n = 12), 63.2 ± 13.7 ms in control (n = 34; P = 0.014, unpaired t test, comparison to CL), and 66.1 ± 9.2 ms in CD photoreceptors (n = 8; P = 0.007, unpaired t test, comparison to CL). *, P < 0.05; **, P < 0.01; error bars indicate SD.

and photoreceptors of the two other groups (Fig. 3). Fig. 3 (A–C) shows examples of current and voltage bump responses to low-intensity continuous illumination in the same CL, control, and CD photoreceptors. Voltage bumps in CL photoreceptors were much bigger than in control and CD photoreceptors at similar membrane potentials. To compare average voltage bumps, we selected subgroups of photoreceptors so that the average resting potentials were approximately the same for each group (Fig. 3 D). This was done to equalize the effects of voltage-dependent membrane conductances on membrane time constant ($\tau = C_m \cdot R$, where R is total membrane resistance), and therefore, on the amplitude and kinetics of voltage bumps. When the average voltage bumps were normalized, it emerged that voltage bumps in CL rise and decay faster than in control and CD photoreceptors (Fig. 3 E).

Macroscopic light-induced currents

Typical examples of light-induced current (LIC) evoked by 4-s pulses of steady light in 10-fold intensity increments from CL, control, and CD photoreceptors are shown in Fig. 4 A. Average dependencies of sustained LIC on light level are shown in Fig. 4 B. Sustained LIC in CL photoreceptors was significantly smaller than LICs in two other groups at all light backgrounds. It should be noted that many CL photoreceptors had such a low absolute sensitivity that only quantum bumps could be evoked in the brightest light. Such cells with effectively zero macroscopic LIC were included neither in the average of Fig. 4 B nor in the statistical group comparisons presented in the figure legend, so the numbers provided represent substantial overestimates of the population-average LIC in CL photoreceptors.

Although the sustained LIC values in control and CD photoreceptors were not significantly different at intensities 5×10^{-1} and 5×10^{-2} (Fig. 4 B), at still dimmer intensities of 5×10^{-3} and 5×10^{-4}, the sustained LIC recorded from CD photoreceptors was notably higher than LIC in control (Fig. 4 B). These results are consistent with the increased absolute sensitivity of CD photoreceptors. Also consistent with the previous findings, a strong correlation was found between C_m and sustained LIC amplitude at 5×10^{-1} (Fig. 4 C). For the combined CL, control, and CD data, the Spearman's ρ coefficient was −0.64 ($P < 10^{-5}$). Likewise, as can be seen from Table 1, LIC at 5×10^{-1} correlated strongly (ρ = −0.71) with absolute sensitivity at 5×10^{-6}.

Potassium currents

Several voltage-activated K^+ (Kv) currents have been found in *P. americana* photoreceptors, including a transient IA of unknown molecular origin, and a delayed rectifier (IDR) mainly mediated by Eag channels (Immonen et al., 2017). There were only small differences between Kv currents in the three experimental groups. Fig. 5 A shows a representative Kv current recording from a CL photoreceptor. Fig. 5 B compares conductance–voltage relationships for the IDR in CL, control, and CD photoreceptors. Maximal conductance (G_{max}) and half-activation potential values were obtained by fitting the relationships with a sigmoidal function. G_{max} was slightly smaller in CL than in control and CD photoreceptors (Fig. 5 B). These changes in G_{max} values are consistent with the previously reported moderate positive correlations between C_m and G_{max} values (Salmela et al., 2012). Half-activation potential values were not different between the groups.

Information processing

Next, we investigated the effects of chronic light exposure/deprivation on information transfer. A 60-s GWN stimulus was used over a range of light intensities in 10-fold increments. As in the previous patch-clamp studies, dependencies of information rate (IR) on light intensity in control and CD photoreceptors were usually characterized by the presence of a clear IR maximum (IR_{max}) in relatively bright light, with a sharp IR decrease in still brighter light because of saturation of phototransduction (Frolov, 2016). In contrast, because of low sensitivity to light, voltage responses of CL photoreceptors to GWN usually showed no such IR saturation. Fig. 6 A demonstrates typical voltage responses of CL, control, and CD photoreceptors associated with IR_{max}. The voltage noise was the highest in the CL photoreceptor and the lowest in the CD photoreceptor.

Consistent with the differences in LIC (Fig. 4), voltage responses to GWN were characterized by the lowest sustained

Downloaded from http://rupress.org/jgp/article-pdf/150/10/1386/1797456/jgp_201812107.pdf by guest on 09 February 2026

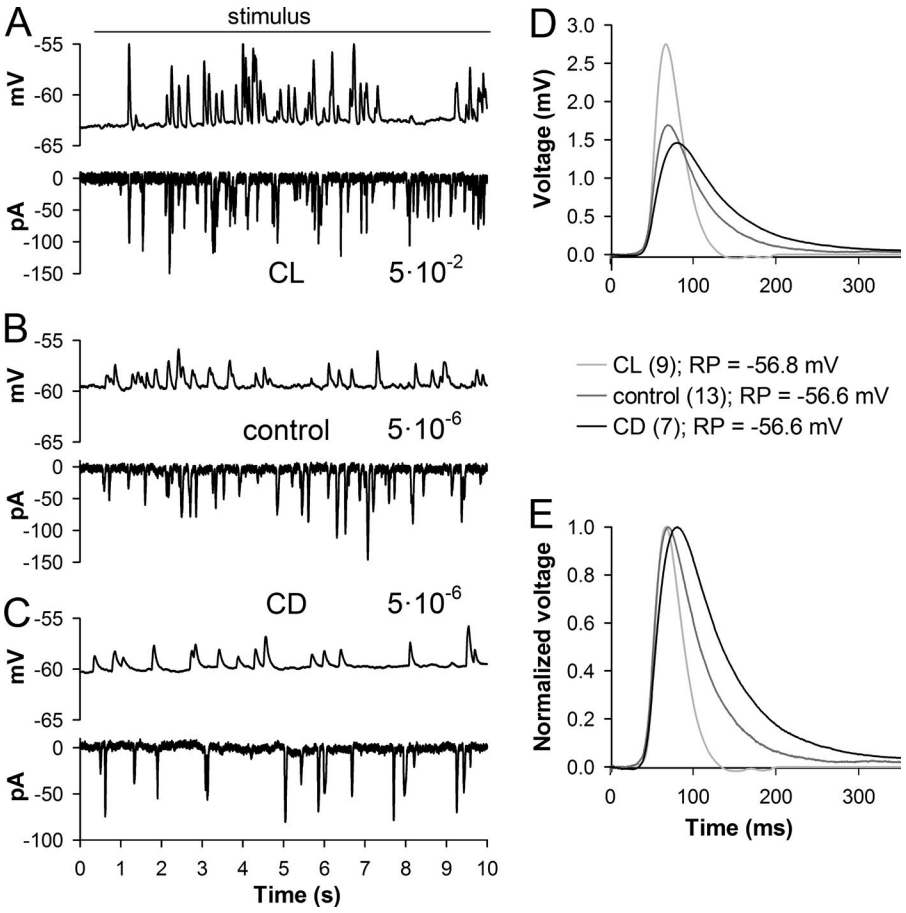

Figure 3. **Elementary current and voltage responses. (A–C)** Typical quantum bump responses to low-intensity continuous light stimulation in each experimental group; voltage and current recordings were obtained from the same photoreceptors using the same stimulation protocol; as shown, stimulus intensities were the same for each recording pair but different between the groups. **(D)** Average voltage bumps. Because of strong dependence of the voltage bump amplitude on resting membrane potential, the voltage bumps were obtained in the following way: first, mean voltage bumps were obtained for each photoreceptor by aligning the rising parts of the bumps; second, a subgroup of cells was selected so that the average resting potentials were approximately the same for all experimental groups. In the subgroups, the mean resting potentials were −56.8 ± 5.3 mV (n = 9) for CL, −56.6 ± 5.6 mV (n = 13) for control, and −56.6 ± 5.5 mV (n = 7) for CD photoreceptors. The corresponding mean C_m values were 156 ± 62, 345 ± 164, and 469 ± 169 pF. **(E)** Normalized voltage bumps from D.

depolarization in CL photoreceptors and the highest in control and CD photoreceptors (Fig. 6 B). When dependencies of IR on background in each photoreceptor were averaged, excluding IR values associated with saturated responses in backgrounds brighter than those eliciting IR_{max} responses (Fig. 6 C), the following picture emerged. First, at all light levels, control and CD photoreceptors transferred significantly more information than CL photoreceptors. Second, in dim backgrounds, CD photoreceptors were characterized by higher information rates than control photoreceptors. For example, at the intermediate light, 5×10^{-3} IR was 8.0 ± 4.0 bits/s in control (n = 21) and 12.3 ± 6.2 bits/s in CD photoreceptors (n = 9, P = 0.03, unpaired t test). This was because of decreased noise in CD relative to control photoreceptors.

Accordingly, IR_{max} values were observed in relatively dim light in control and CD, and in bright light in CL photoreceptors, with more IR_{max} values detected in relatively bright backgrounds in control than in CD photoreceptors (Fig. 6 D). The IR_{max} values were about the same in control and CD but much smaller in CL photoreceptors (Fig. 6 E). However, it should be noted that the mean CL IR_{max} value could be an underestimate because most IR_{max} responses were recorded at the highest light intensity technically feasible in our experiments (Fig. 6 D). It is possible that IRs of such photoreceptors did not reach their maxima and might be higher in still brighter light.

We were interested in differences in information processing between the three groups at the peak of their photoreceptor performance. We therefore compared signal gain, signal power, and noise power functions in the frequency domain for the responses associated with IR_{max}. Median dependencies of signal gain on frequency are shown in Fig. 7 A. The values of 3-dB membrane "corner" frequencies (f_{3dB}) were obtained by fitting IR_{max} signal gain functions in each photoreceptor with a first-order Lorentzian function. The values of f_{3dB} were twice as high in CL as in control and CD photoreceptors (Fig. 7 B). Median frequency-dependencies of signal and noise power for responses associated with IR_{max} are shown in Fig. 7 C. Consistently with the weaker low-pass filtering, signal power was higher in CL than in control or CD photoreceptors in the higher-frequency region. However, because of the opposite tendencies in the lower-frequency region and a rapid decrease in signal power with frequency, total signal power for any of the three conditions was not statistically different (Fig. 7 D). Consistent with the increased voltage bump noise, the total noise power was significantly higher in CL than in control and CD photoreceptors (Fig. 7 D). Because of high noise, the median signal-to-noise ratio (SNR) function for CL was smaller than the SNR functions for control and CD photoreceptors (Fig. 7 E).

Changes in gene expression

We also investigated the expression of genes encoding some proteins important for phototransduction. Quantitative PCR analysis of the mRNA levels for three opsins and two light-activated channels, which were previously identified in the cockroach retina (French et al., 2015; Saari et al., 2017), found that the mean

Downloaded from http://rupress.org/jgp/article-pdf/150/10/1386/1797456/jgp_201812107.pdf by guest on 09 February 2026

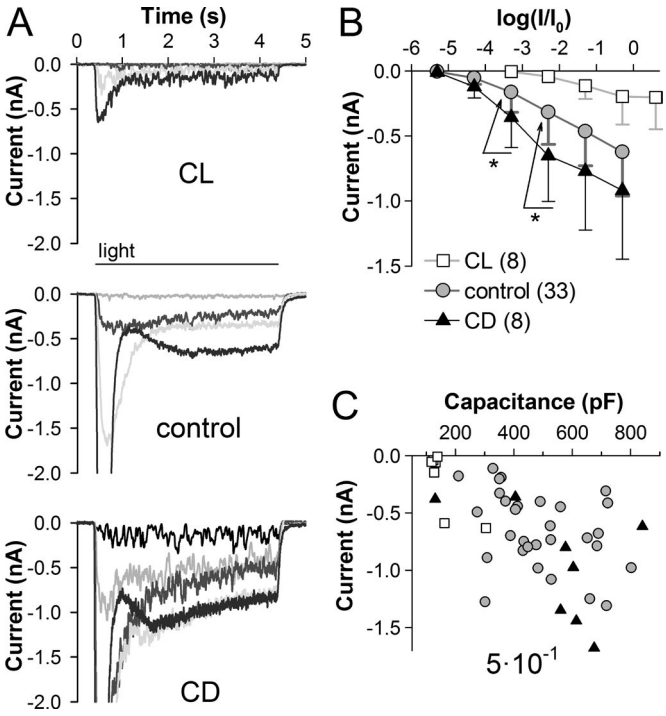

Figure 4. **Macroscopic light-induced currents. (A)** Typical light-induced currents recorded from CL, control, and CD photoreceptors; 4-s light stimuli were used at six (in control and CD photoreceptors) or seven (in CL photoreceptors) intensities in 10-fold increments; stimulus duration is shown as a horizontal bar. **(B)** Dependence of sustained LIC on light intensity; the values were obtained as averages of the final 3 s of current responses; although not all data samples passed the normality test, the data here for presentation purposes are shown as mean ± SD; error bars are shown in the negative direction. At all intensities, LIC in CL photoreceptors was significantly smaller than LIC in control and CD photoreceptors. For example, at light intensity 5×10^{-1}, sustained LIC amplitudes were −165 (−429:−46) pA in CL (n = 8), −555 (−787:−348) pA in control (n = 34; P = 0.0014, MWUT, comparison with CL), and −887 (−1,339:−540) pA in CD (n = 8; P = 0.014, MWUT, comparison with CL). LIC values in control and CD photoreceptors were not significantly different from each other at intensities 5×10^{-1} and 5×10^{-2} (P = 0.11 and 0.09, respectively, MWUT). However, in relatively dim light, LIC in CD photoreceptors exceeded that in control: at intensity 5×10^{-3}, the sustained LIC amplitudes were −260 (−458:−111) pA in control (n = 34) versus −517 (−795:−395) pA in CD (n = 8; P = 0.019, MWUT); at 5×10^{-4}, the sustained LIC amplitudes were −103 (−285:−25) pA in control (n = 33) versus −373 (−545:−135) pA in CD (n = 8; P = 0.015, MWUT). *, P < 0.05. **(C)** Correlations between the amplitudes of sustained LIC and C_m values at intensity 5×10^{-1}.

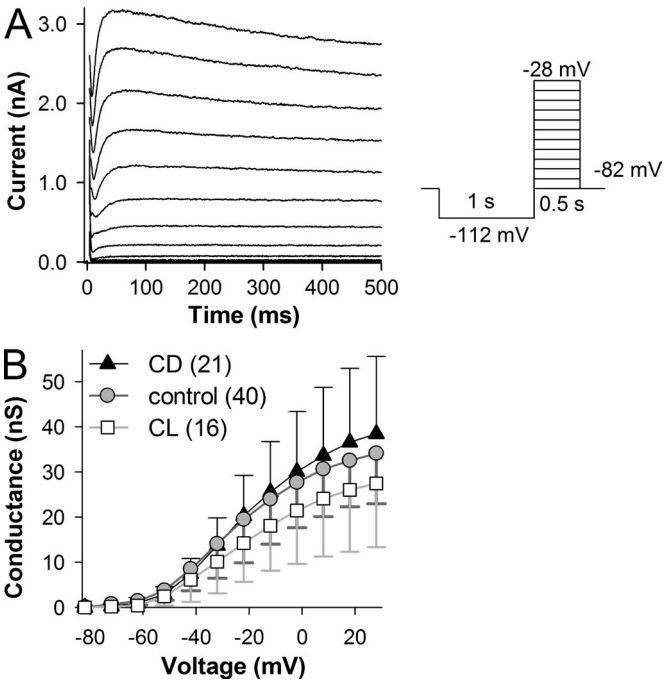

Figure 5. **Potassium currents. (A)** A typical Kv current recorded from a photoreceptor after CL exposure; the recording protocol is shown to the right; each testing step was preceded by a 1-s prepulse to −102 mV to fully recover the transient IA; the first 3 ms of the current traces containing capacitive transients were removed. **(B)** Current–voltage relationships for sustained Kv conductance in CL, control, and CD photoreceptors; values are averages of final 200 ms for each trace; data points were fitted with a sigmoidal function; standard deviation bars are shown in different directions for presentation purposes. G_{max} was slightly smaller in CL than in control and CD photoreceptors: 29.1 ± 14.9 nS (n = 16), 37.3 ± 13.0 nS (n = 40; P = 0.066, t test, comparison with CL), and 40.5 ± 17.8 nS (n = 21; P = 0.041, t test, comparison with CL), respectively.

expression of the dominant green-sensitive opsin (GO1) was strongly up-regulated in CD retinas (Fig. 8). This appears to be the photoreceptors' primary response to light deprivation and contributes to their improved light sensitivity. GO2 and UVO may be less important for cockroach vision in visible light, because their expression decreased during long-term light deprivation. Both cation channels that are required for transduction in cockroach photoreceptors, TRP and TRPL, were slightly down-regulated in CD retinas, suggesting that lack of a functioning transduction cascade reduced their expression. However, the large amount of GO1 still resulted in higher sensitivity and longer-lasting responses. Expression of the Gq protein that mediates TRP and TRPL signaling and Arrestin (Arr) that terminates rhodopsin signaling and halts Gq production were decreased in CD but not in CL photoreceptors. Expression of phospholipase C (PLC), which is activated by the Gq, was unchanged in both experimental conditions. Overstimulation by CL slightly up-regulated GO1, GO2, Arr, and TRPL, resulting in faster and more transient responses but lower absolute sensitivity than control.

Discussion

In this work, we investigated the effects of long-term exposure to bright light or chronic light deprivation on photoreceptor properties and function in the nocturnal insect *P. americana*. This is the first study of phenotypic plasticity of microvillar photoreceptors other than dipterans, and its results are only partly consistent with findings in flies (Deimel and Kral, 1992; Wolfram and Juusola, 2004).

Distinct combinations of electrophysiological adaptations were found in CL-exposed and CD-exposed photoreceptors. In comparison to control, CL photoreceptors were characterized by reduced membrane capacitance, sensitivity to light, sustained light-induced and voltage-activated K^+ currents, latency of phototransduction, sustained depolarization, and maximal information rate. They also exhibited enlarged voltage bumps, voltage bump noise, and membrane corner frequency. All these

Downloaded from http://rupress.org/jgp/article-pdf/150/10/1386/1797456/jgp_201812107.pdf by guest on 09 February 2026

Table 1. **Spearman's rank order correlation coefficients for the combined CL, control, and CD data**

	C_m	Absolute sensitivity	LIC at 5 x 10^{-1}	IR_{max}
Absolute sensitivity	−0.84 (10^{-6})			
LIC at 5 × 10^{-1}	−0.64 (10^{-5})	−0.71 (10^{-5})		
IR_{max}	0.36 (0.03)	0.71 (10^{-5})	−0.73 (10^{-6})	
f_{3dB}	−0.49 (0.003)	−0.45 (0.03)	0.28 (0.16)	0.01 (0.95)

Numbers in parentheses denote P values; low values indicate statistically significant correlations. For all correlations, the number of data points was >30.

parameters changed in the opposite directions in CD photoreceptors. However, differences between CD and control photoreceptors were smaller than those between CL and controls. For instance, sustained light-induced current was significantly larger in CD than in control photoreceptors in relatively dim light (Fig. 4), whereas in bright light the relative difference was smaller. Although this could be explained by the relatively small experimental group sizes and the intrinsically high variability in the *Periplaneta* photoreceptor properties (Heimonen et al., 2006), it is more likely that this reflects the sensitivity-boosting adaptations in CD photoreceptors (see below), which simultaneously increased the total light-induced current in dim light. On the other hand, in bright light, Ca^{2+}-dependent light adaptation (Immonen et al., 2014) could have a stronger suppressing effect on light-induced current in CD than in control photoreceptors. These observations are also in line with the finding of higher information rates in CD than in control in relatively dim backgrounds (Fig. 6 C), indicative of shifting operational ranges of photoreceptors in the three experimental groups.

The changes seen in photoreceptors exposed to CL clearly facilitated faster and more broadband signal processing at the expense of sensitivity to light, whereas the light-deprived photoreceptors favored absolute sensitivity by larger rhabdom area and a surge in expression of green opsin. A consequence of the enlarged rhabdom reflected in higher capacitance was the finding of slower voltage responses. These observations are fully consistent with the classic visual ecological paradigm explaining physiological differences in photoreceptor functioning between diurnal and nocturnal species as a result of sensitivity/speed trade-offs (Weckström and Laughlin, 1995; Cronin et al., 2014). However, it should be noted that CL photoreceptors were not able to eliminate the excessive voltage noise, which prevented translation of expanded bandwidth into superior information capacity (see below).

Plasticity in *P. americana* photoreceptors

Our results indicate that the differences between the experimental groups originate from two independent sources: extensive changes in the size of the rhabdom and intensive changes in the speed of phototransduction.

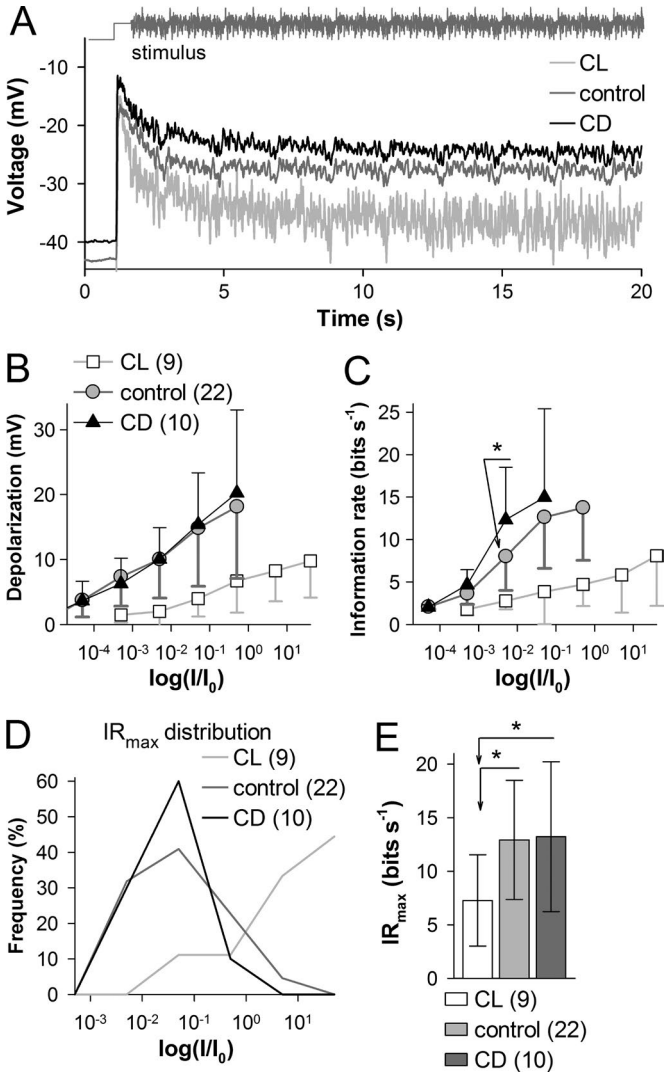

Figure 6. **Responses to Gaussian white noise–modulated light stimuli. (A)** First 20 s of representative voltage responses to a 60-s GWN stimulus at light intensities that elicited IR_{max} responses in photoreceptors kept in CL, control, and CD; the stimulus is shown above. **(B)** Mean sustained membrane depolarizations during responses to GWN at different light intensities; values were obtained by averaging the entire duration of the response except for the first second and then subtracting the resting potential; error bars in B, C, and E denote SD. **(C)** Dependencies of mean IR on light background; in each photoreceptor, IR values associated with saturated responses in relatively bright light, which were smaller than IR_{max}, were excluded; the number of data points varied from 2 (for CL in two dimmest levels) to 21. At all light levels, control and CD photoreceptors transferred significantly more information than CL photoreceptors ($P < 10^{-3}$ for all comparisons, values not shown). *, $P < 0.05$. **(D)** Distributions of IR_{max} values depending on light level. **(E)** Average maximal information rates. The IR_{max} values were 7.3 ± 4.3 bits/s in CL ($n = 9$), 12.9 ± 5.6 bits/s in control ($n = 22$; $P = 0.008$ for comparison with CL, unpaired t test), and 13.7 ± 7.3 bits/s in CD photoreceptors ($n = 10$; $P = 0.039$ for comparison with CL, unpaired t test). *, $P < 0.05$.

We have previously shown that the variability in photoreceptor size of several insect species as approximated by membrane capacitance is strongly linked to variabilities in the absolute sensitivity, amplitude of macroscopic sustained light-induced current, membrane corner frequency, and maximal information rate (Frolov, 2016). Moreover, moderate to strong positive cor-

Downloaded from http://rupress.org/jgp/article-pdf/150/10/1386/1797456/jgp_201812107.pdf by guest on 09 February 2026

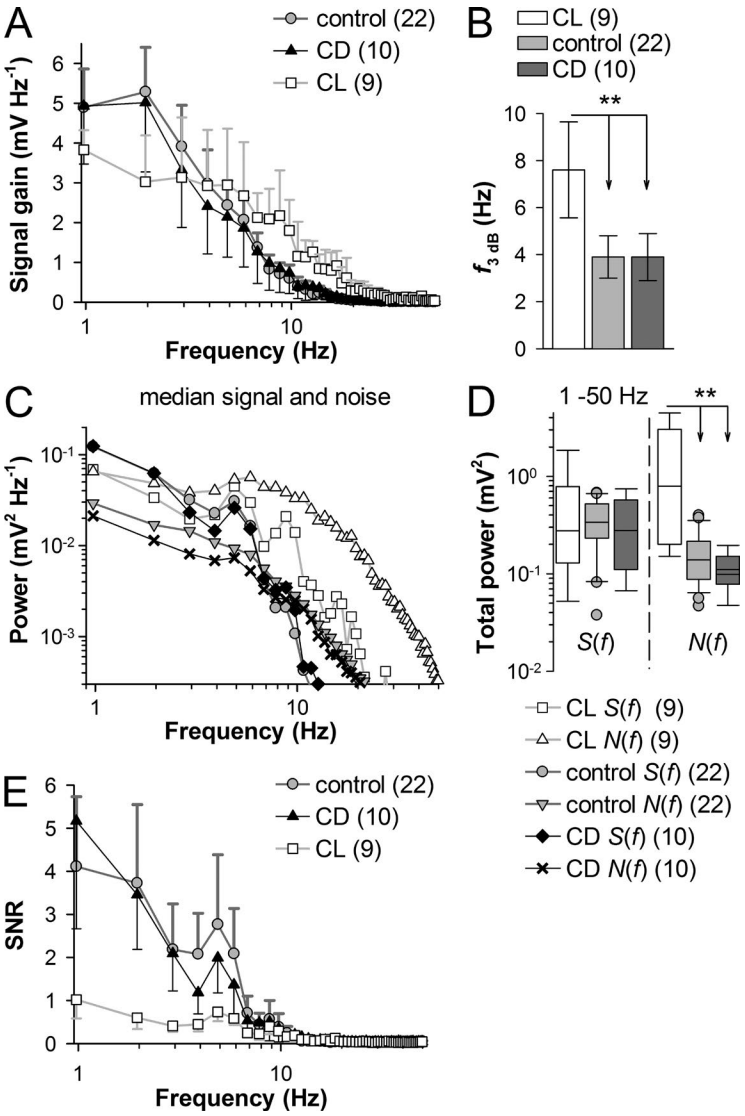

Figure 7. **Information processing for responses associated with IR_{max}. (A)** Median signal gain functions obtained from IR_{max} responses to GWN in CL, control, and CD photoreceptors; in A and E, error bars represent m.a.d. and are shown in different directions for presentation purposes. Dependencies of IR_{max} responses on light level are shown in Fig. 6 D. **(B)** Mean membrane corner frequencies obtained by fitting signal gain functions of IR_{max} responses with a first-order Lorentzian equation. The values of f_{3dB} were 7.6 ± 2.0 Hz in CL (n = 9), 3.8 ± 0.9 Hz in control (n = 22; $P < 10^{-4}$ for comparison with CL, unpaired t test), and 3.9 ± 1.0 Hz in CD photoreceptors (n = 10; $P < 0.001$ for comparison with CL, unpaired t test); error bars denote SD. The legend under B also refers to D. **, $P < 0.01$. **(C)** Median signal and noise power spectra; the legend is under D; error bars are omitted for presentation purposes. **(D)** Box plots compare total signal and noise power spectra integrals in the 1–50-Hz range. The total noise power was significantly higher in CL than in control and CD photoreceptors: in the range from 1 to 50 Hz, it was 0.87 (0.23:1.89) mV^2 in CL (n = 9; P = 0.008 and 0.001, MWUT, for comparison with control and CD, respectively), 0.13 (0.09:0.18) mV^2 in control (n = 22), and 0.12 (0.10:0.16) mV^2 in CD photoreceptors (n = 10). **, $P < 0.01$. **(E)** Median SNR functions.

relations were found for various combinations of these parameters (Table 1). Although correlation does not necessarily mean causation, the common factor of rhabdom size underlies all these parameters. If membrane capacitance is mainly determined by the rhabdom area, this would explain the correlations between capacitance and absolute sensitivity, and between capacitance and sustained light-induced current. On the other hand, information rate depends on the number of microvilli, the photoreceptor's sampling units, which is also reflected in membrane capacitance, albeit indirectly.

The area of light-sensitive membrane is directly proportional to the number of microvilli and, together with the somatic and axonal membrane, contributes to the capacitance. Axonal membrane is absent in the dissociated ommatidia. In *P. americana*, using data from previous transmission electron microscopy studies (Frolov et al., 2017) and our unpublished observations indicating that the ommatidium is two tiered, the soma can be approximated by a cylinder of 10 µm in diameter and 100 µm in length, whereas the microvillus has a diameter of 68 nm and average length of ∼3 µm. Disregarding the flanking surfaces and assuming that the photoreceptor contains 30,000 microvilli (a *Drosophila* estimate, much lower than the *P. americana* estimate; Frolov et al., 2017) gives ∼3,100 μm^2 of the somatic membrane and 19,000 μm^2 of the rhabdomeric membrane.

How much of the membrane area can be captured in capacitive transients in voltage-clamp experiments considering that the photoreceptor is a slender cell containing tens of thousands of even more slender microvilli? To determine potential contribution of incomplete space-clamp to underestimation of whole-cell capacitance, the following calculations were performed. The validity of capacitance measurements in approximating the size of the photoreceptor depends on whether the cell can be considered isopotential. Our recordings were performed on dissociated ommatidia lacking axons. Under such conditions, the photoreceptor can be represented by two compartments: the soma and the rhabdomere. Calculation of length constant for the soma using a relatively low specific membrane resistivity of 1 kΩ·cm^2 and a normal specific intracellular resistivity of 200 Ω·cm gives a length constant of 350 µm. The microvillus has internal diameter of ∼60 nm. Disregarding the resistivity of the extracellular space and using the specific membrane and intracellular resistivity values above yields a length constant of 27 µm. Consider-

Downloaded from http://rupress.org/jgp/article-pdf/150/10/1386/1797456/jgp_201812107.pdf by guest on 09 February 2026

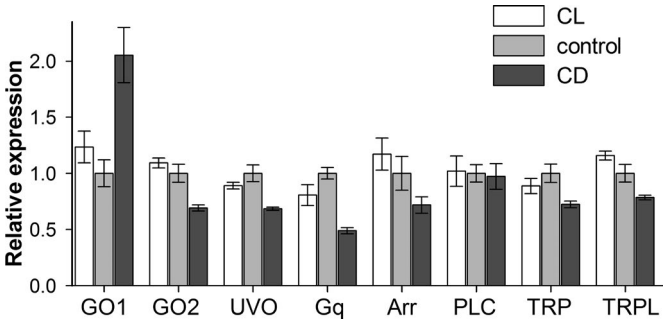

Figure 8. **qPCR results for gene expression.** Relative expression of *GO1*, *UVO*, *GO2*, *Gq*, *Arr*, *PLC*, *TRP*, and *TRPL* mRNA from CL, control, and CD retinas; data were obtained by qPCR and normalized to reference genes for *actin* and *GAPDH*. Values represent means ± SEM of three technical replicates of testing the same experimental samples as described in Materials and methods.

ing the very narrow extracellular space between microvilli, and assuming a 5-nm distance between neighboring microvilli and specific intracellular and extracellular resistivity of 300 Ω·cm, yields a microvillus length constant of ∼8 µm. These estimates indicate that when ion channels are closed in the dark at the resting potential, strongly increasing specific membrane resistivity, both the soma and the rhabdomere in *P. americana* can be considered isopotential.

In *Drosophila* photoreceptors, voltage-activated K^+ channels were shown to be expressed in the soma, with delayed rectifier Shab channels found at the microvillar bases (Rogero et al., 1997; Hardie and Raghu, 2001). We previously showed for *Periplaneta* and several other species that although delayed rectifier K^+ conductance correlates positively with membrane capacitance, such correlations are usually much weaker than between capacitance and light-induced current. This implies that the delayed rectifier and light-activated channels are situated in different compartments (Frolov, 2016). Here we also showed that the changes in sustained K^+ conductance are much smaller than the corresponding changes in light-induced current (Fig. 5). This is consistent with both the extra-rhabdomeric localization of the K^+ channels and the hypothesis that the main changes occur in the rhabdom. It should be noted that the physical dimensions of dissociated ommatidia in all three experimental groups were similar.

The changes in capacitance directly affected two major aspects of information processing: membrane corner frequency and noise power. The former is determined by a product of membrane capacitance and momentary resistance, which mainly depends on sustained K^+ conductance. As we demonstrated here, changes in capacitance were accompanied by disproportionally smaller changes in the K^+ conductance. This significantly increased corner frequency in CL photoreceptors and improved transfer of higher-frequency components of the stimulus (Fig. 6 D). However, all possible advantages of such signal power redistribution (Fig. 7 A) were negated by a drastically increased voltage noise (Fig. 7, B and C) because of large voltage bumps (Fig. 3), which are also caused by reduced low-pass filtering. Why then do fly photoreceptors, characterized by relatively small capacitances (Frolov et al., 2016), not demonstrate such high-voltage noise? One reason could be that, in contrast to *Periplaneta*, fly photoreceptors express relatively few high-conductance TRPL channels. In contrast, we previously found that knockdown of the TRPL gene causes a dramatic reduction in voltage noise in cockroach photoreceptors (Saari et al., 2017). Accordingly, here we found a small increase in the TRPL expression in CL retinas and an increase in voltage noise (Fig. 8).

Changes in phototransduction manifested in the decrease of mean bump latency by ∼14% in CL photoreceptors and in a small increase in CD photoreceptors (Fig. 2). Decreased latency is associated with a smaller dispersion of quantum bumps in response to a flash of light and therefore with better temporal resolution of a contrast-modulated stimulus by the photoreceptor membrane, and vice versa (Wolfram and Juusola, 2004). Faster phototransduction and voltage responses are strongly associated with diurnal, fast-flying, maneuverable species (Weckström and Laughlin, 1995; Frolov, 2016). As quantum bump latency is thought to be mainly determined by molecular events during the first part of phototransduction cascade (Wolfram and Juusola, 2004), the reduced expression of Gq and Arr (Fig. 8) seems to be consistent with the slightly increased latency in CD photoreceptors.

Periplaneta versus *Drosophila*

The effects of rearing *Drosophila* under normal illumination (a 12-h light/12-h dark cycle) versus in the dark for several generations were previously investigated for changes in photoreceptor properties (Wolfram and Juusola, 2004). Intracellular recordings from photoreceptors were performed between days 2 and 10 after eclosion. In light-reared flies, the following changes were observed in comparison to dark-reared flies: a significant decrease in input resistance without effects on capacitance, accelerated light response, lower sustained depolarization, slightly increased signal and noise power, decreased membrane time constant, and higher information rate. These adaptations can be explained by acceleration of phototransduction and increased membrane leak conductance. In addition, the authors investigated the effects of short-term (2-h) exposure to either light or darkness in both experimental groups before recordings and found that such interventions substantially modify the original photoreceptor phenotypes.

Although some changes reported in *Drosophila* are similar to our findings, others are not. We did not observe any effect of light/dark rearing on input resistance. In contrast, although membrane capacitance was not altered in *Drosophila*, it was drastically changed in *Periplaneta*. Changes in signal and noise power spectra, and in membrane corner frequency, were quite similar, although noise increased more in *Periplaneta* CL photoreceptors than in light-reared fruit flies. Because of this, information rate decreased in *Periplaneta* CL but increased in light-reared *Drosophila*. Phototransduction was accelerated both in CL cockroaches and light-reared flies in comparison to the respective controls. Therefore, although the adaptive changes in *Drosophila*, e.g., in input resistance, appear to be mainly functional, the changes in *Periplaneta* associated with C_m seem to be caused by predominantly structural modifications. However, comparing the results of these two studies is problematic because of differing methodologies: in the *Drosophila* study, rearing under dissimilar conditions for few generations may not produce

Downloaded from http://rupress.org/jgp/article-pdf/150/10/1386/1797456/jgp_201812107.pdf by guest on 09 February 2026

major changes between the groups (but see Izutsu et al., 2012) if it is the individual history that matters. In the case of fruit flies, this history includes larval and young adult exposure to light or dark. Moreover, the duration of long-term light exposure of the adult photoreceptors was not controlled for, as recordings were performed between days 2 and 10 after eclosion. The relatively short *Drosophila* life span and practical difficulties with recording from older flies preclude longer experiments like those on mature photoreceptors presented here.

Conclusions

We studied changes in photoreceptor function in *P. americana* after prolonged exposure to strongly differing illumination conditions. Chronic and drastic alterations in the visual input elicited distinct and opposing patterns of functional adjustments. Our data indicate that most of the long-term light-driven adaptations in *Periplaneta* can be linked to changes in the size of rhabdom that effectively adjust photoreceptor function to new environmental conditions.

Acknowledgments

This research was supported by the Natural Sciences and Engineering Research Council of Canada grants RGPIN/5565 (to P.H. Torkkeli) and RGPIN/03712 (to A.S. French).

The authors declare no competing financial interests.

Author contributions: R.V. Frolov: conceptualization, electrophysiology, data analysis, manuscript writing, review, and editing; E.-V. Immonen: electrophysiology; P. Saari: manuscript review and editing; H. Liu: quantitative PCR experiments; P.H. Torkkeli and A.S. French: interpretation of the data, project administration, manuscript writing, and editing.

Richard W. Aldrich served as editor.

Submitted: 26 April 2018
Revised: 4 July 2018
Accepted: 31 July 2018

References

Bähner, M., S. Frechter, N. Da Silva, B. Minke, R. Paulsen, and A. Huber. 2002. Light-regulated subcellular translocation of Drosophila TRPL channels induces long-term adaptation and modifies the light-induced current. *Neuron.* 34:83–93. https://doi.org/10.1016/S0896-6273(02)00630-X

Barth, M., H.V. Hirsch, I.A. Meinertzhagen, and M. Heisenberg. 1997. Experience-dependent developmental plasticity in the optic lobe of Drosophila melanogaster. *J. Neurosci.* 17:1493–1504. https://doi.org/10.1523/JNEUROSCI.17-04-01493.1997

Berry, K.P., and E. Nedivi. 2016. Experience-dependent structural plasticity in the visual system. *Annu. Rev. Vis. Sci.* 2:17–35. https://doi.org/10.1146/annurev-vision-111815-114638

Brann, M.R., and L.V. Cohen. 1987. Diurnal expression of transducin mRNA and translocation of transducin in rods of rat retina. *Science.* 235:585–587. https://doi.org/10.1126/science.3101175

Calvert, P.D., K.J. Strissel, W.E. Schiesser, E.N. Pugh Jr., and V.Y. Arshavsky. 2006. Light-driven translocation of signaling proteins in vertebrate photoreceptors. *Trends Cell Biol.* 16:560–568. https://doi.org/10.1016/j.tcb.2006.09.001

Carey, J.R. 2001. Insect biodemography. *Annu. Rev. Entomol.* 46:79–110. https://doi.org/10.1146/annurev.ento.46.1.79

Cronin, M.A., M.H. Lieu, and S. Tsunoda. 2006. Two stages of light-dependent TRPL-channel translocation in Drosophila photoreceptors. *J. Cell Sci.* 119:2935–2944. https://doi.org/10.1242/jcs.03049

Cronin, T.W., S. Johnsen, N.J. Marshall, and E.J. Warrant. 2014. Visual Ecology. Princeton, NJ: Princeton University Press

Deimel, E., and K. Kral. 1992. Long-term sensitivity adjustment of the compound eyes of the housefly Musca domestica during early adult life. *J. Insect Physiol.* 38:425–430. https://doi.org/10.1016/0022-1910(92)90119-X

Fain, G.L., R. Hardie, and S.B. Laughlin. 2010. Phototransduction and the evolution of photoreceptors. *Curr. Biol.* 20:R114–R124. https://doi.org/10.1016/j.cub.2009.12.006

Frechter, S., and B. Minke. 2006. Light-regulated translocation of signaling proteins in Drosophila photoreceptors. *J. Physiol. Paris.* 99:133–139. https://doi.org/10.1016/j.jphysparis.2005.12.010

French, A.S., S. Meisner, H. Liu, M. Weckström, and P.H. Torkkeli. 2015. Transcriptome analysis and RNA interference of cockroach phototransduction indicate three opsins and suggest a major role for TRPL channels. *Front. Physiol.* 6:207. https://doi.org/10.3389/fphys.2015.00207

Frolov, R.V. 2015. Biophysical properties of photoreceptors in Corixa punctata facilitate diurnal life-style. *Vision Res.* 111(Pt A):75–81. https://doi.org/10.1016/j.visres.2015.03.026

Frolov, R.V. 2016. Current advances in invertebrate vision: insights from patch-clamp studies of photoreceptors in apposition eyes. *J. Neurophysiol.* 116:709–723. https://doi.org/10.1152/jn.00288.2016

Frolov, R., E.V. Immonen, M. Vähäsöyrinki, and M. Weckström. 2012. Postembryonic developmental changes in photoreceptors of the stick insect Carausius morosus enhance the shift to an adult nocturnal life-style. *J. Neurosci.* 32:16821–16831. https://doi.org/10.1523/JNEUROSCI.2612-12.2012

Frolov, R., E.V. Immonen, and M. Weckstrom. 2016. Visual ecology and potassium conductances of insect photoreceptors. J. Neurophysiol.115:2147–2157.

Frolov, R.V., A. Matsushita, and K. Arikawa. 2017. Not flying blind: a comparative study of photoreceptor function in flying and non-flying cockroaches. *J. Exp. Biol.* 220:2335–2344. https://doi.org/10.1242/jeb.159103

Hardie, R.C., and P. Raghu. 2001. Visual transduction in Drosophila. *Nature.* 413:186–193. https://doi.org/10.1038/35093002

Heimonen, K., I. Salmela, P. Kontiokari, and M. Weckström. 2006. Large functional variability in cockroach photoreceptors: optimization to low light levels. *J. Neurosci.* 26:13454–13462. https://doi.org/10.1523/JNEUROSCI.3767-06.2006

Hertel, H. 1983. Change of synapse frequency in certain photoreceptors of the honeybee after chromatic deprivation. *J. Comp. Physiol.* 151:477–482. https://doi.org/10.1007/BF00605464

Hubel, D.H., and T.N. Wiesel. 1970. The period of susceptibility to the physiological effects of unilateral eye closure in kittens. *J. Physiol.* 206:419–436. https://doi.org/10.1113/jphysiol.1970.sp009022

Hubel, D.H., T.N. Wiesel, and S. LeVay. 1977. Plasticity of ocular dominance columns in monkey striate cortex. *Philos. Trans. R. Soc. Lond. B Biol. Sci.* 278:377–409. https://doi.org/10.1098/rstb.1977.0050

Immonen, E.V., S. Krause, Y. Krause, R. Frolov, M.T. Vähäsöyrinki, and M. Weckström. 2014. Elementary and macroscopic light-induced currents and their Ca(2+)-dependence in the photoreceptors of Periplaneta americana. *Front. Physiol.* 5:153. https://doi.org/10.3389/fphys.2014.00153

Immonen, E.V., A.S. French, P.H. Torkkeli, H. Liu, M. Vähäsöyrinki, and R.V. Frolov. 2017. EAG channels expressed in microvillar photoreceptors are unsuited to diurnal vision. *J. Physiol.* 595:5465–5479. https://doi.org/10.1113/JP273612

Izutsu, M., J. Zhou, Y. Sugiyama, O. Nishimura, T. Aizu, A. Toyoda, A. Fujiyama, K. Agata, and N. Fuse. 2012. Genome features of "Dark-fly", a Drosophila line reared long-term in a dark environment. *PLoS One.* 7:e33288. https://doi.org/10.1371/journal.pone.0033288

Jiang, J., W. Zhu, F. Shi, Y. Liu, J. Li, W. Qin, K. Li, C. Yu, and T. Jiang. 2009. Thick visual cortex in the early blind. *J. Neurosci.* 29:2205–2211. https://doi.org/10.1523/JNEUROSCI.5451-08.2009

Laughlin, S.B. 1989. The role of sensory adaptation in the retina. *J. Exp. Biol.* 146:39–62.

Meinertzhagen, I.A. 1989. Fly photoreceptor synapses: their development, evolution, and plasticity. *J. Neurobiol.* 20:276–294. https://doi.org/10.1002/neu.480200503

Pallas, S.L. 2017. The impact of ecological niche on adaptive flexibility of sensory circuitry. *Front. Neurosci.* 11:344. https://doi.org/10.3389/fnins.2017.00344

Rogero, O., B. Hämmerle, and F.J. Tejedor. 1997. Diverse expression and distribution of Shaker potassium channels during the development of the

Downloaded from http://rupress.org/jgp/article-pdf/150/10/1386/1797456/jgp_201812107.pdf by guest on 09 February 2026

Drosophila nervous system. *J. Neurosci.* 17:5108–5118. https://doi.org/10.1523/JNEUROSCI.17-13-05108.1997

Rudolf, J., A. Meglič, G. Zupančič, and G. Belušič. 2014. Development and plasticity of mitochondria and electrical properties of the cell membrane in blowfly photoreceptors. *J. Comp. Physiol. A Neuroethol. Sens. Neural Behav. Physiol.* 200:669–680. https://doi.org/10.1007/s00359-014-0912-4

Saari, P., A.S. French, P.H. Torkkeli, H. Liu, E.V. Immonen, and R.V. Frolov. 2017. Distinct roles of light-activated channels TRP and TRPL in photoreceptors of *Periplaneta americana*. *J. Gen. Physiol.* 149:455–464. https://doi.org/10.1085/jgp.201611737

Salmela, I., E.V. Immonen, R. Frolov, S. Krause, Y. Krause, M. Vähäsöyrinki, and M. Weckström. 2012. Cellular elements for seeing in the dark: voltage-dependent conductances in cockroach photoreceptors. *BMC Neurosci.* 13:93. https://doi.org/10.1186/1471-2202-13-93

Sokolov, M., A.L. Lyubarsky, K.J. Strissel, A.B. Savchenko, V.I. Govardovskii, E.N. Pugh Jr., and V.Y. Arshavsky. 2002. Massive light-driven translocation of transducin between the two major compartments of rod cells: a novel mechanism of light adaptation. *Neuron.* 34:95–106. https://doi.org/10.1016/S0896-6273(02)00636-0

Voolstra, O., E. Rhodes-Mordov, B. Katz, J.P. Bartels, C. Oberegelsbacher, S.K. Schotthöfer, B. Yasin, H. Tzadok, A. Huber, and B. Minke. 2017. The phosphorylation state of the *Drosophila* TRP channel modulates the frequency response to oscillating light *in vivo*. *J. Neurosci.* 37:4213–4224. https://doi.org/10.1523/JNEUROSCI.3670-16.2017

Wagner, H.J., and R.H. Kröger. 2005. Adaptive plasticity during the development of colour vision. *Prog. Retin. Eye Res.* 24:521–536. https://doi.org/10.1016/j.preteyeres.2005.01.002

Weckström, M., and S.B. Laughlin. 1995. Visual ecology and voltage-gated ion channels in insect photoreceptors. *Trends Neurosci.* 18:17–21. https://doi.org/10.1016/0166-2236(95)93945-T

Wolfram, V., and M. Juusola. 2004. Impact of rearing conditions and short-term light exposure on signaling performance in Drosophila photoreceptors. *J. Neurophysiol.* 92:1918–1927. https://doi.org/10.1152/jn.00201.2004

Yamoah, E.N., S. Levic, J.B. Redell, and T. Crow. 2005. Inhibition of conditioned stimulus pathway phosphoprotein 24 expression blocks the reduction in A-type transient K+ current produced by one-trial in vitro conditioning of Hermissenda. *J. Neurosci.* 25:4793–4800. https://doi.org/10.1523/JNEUROSCI.5256-04.2005

Downloaded from http://rupress.org/jgp/article-pdf/150/10/1386/1797456/jgp_201812107.pdf by guest on 09 February 2026